Indian Journal of Pure & Applied Physics
Vol. 57, July 2019, pp. 466-474

Enhanced photodegradation of methylene blue by silica coated ZnSe nanoparticles

M Verma*, K B Sharma & N S Saxena

Semi-conductor and Polymer Science Laboratory, Department of Physics, University of Rajasthan, Jaipur 302 004, India

Received 17 April 2017; accepted 29 April 2019

Herein, we report synthesis of silica-coated ZnSe nanoparticles (SZNPs), by varying the mass to volume ratio of ZnSe : TEOS i.e. mass to mass ratio of ZnSe : SiO_2 ranging from 0.0267 to 0.1071. These SZNPs showed enhanced photodegradation of methylene blue (MB) solution under visible light. Silica coating on ZnSe NPs reduces the toxicity concerns for its wide use as photocatalyst. XRD of bare ZnSe NPs confirms hexagonal crystal structure, and TEM depicts size range of SZNPs around 7 nm. FTIR and Raman measurements confirm the presence of different chemical and silanol groups attached to bare ZnSe and SZNPs. Optical absorption and photoluminescence (PL) show a red shift due to silica coating on ZnSe NPs compared to bare ZnSe. This is due to silanization of ZnSe, as silica shell reduces the recombination of photon-generated electron and hole pairs. Photocatalytic experiments on methylene blue (MB) by bare and SZNPs have been conducted, optimal SZNPs i.e. 0.0535 sample (mass ratio of ZnSe:SiO_2) exhibits enhanced photo-generated free radicals. An increase in photodegradation of SZNPs, i.e. from 35 to 46% has been observed compared to bare counterparts (ZnSe). Stability decreased by only 7% after 4th cycle of reuse, depicting efficacy of the SZNPs photocatalyst in the degradation of MB. A pseudo-first-order reaction kinetics has been observed for photodegradation of MB with highest rate constant of 8.6×10^{-3} min^{-1} for SZNPs (1.0000:0.0535) sample.

Keywords: ZnSe, Photodegradation, Adsorption, Free radical

1 Introduction

Fast economic growth and industrialization have led to the production of pollutants/harmful organic chemicals as by product, which when discharged directly to the environment contaminates water, soil etc. thus creating health issues[1, 2]. Photocatalyst a class of solar energy driven materials exploits the energy of solar radiation to convert the pollutants into non-toxic components by a production of H_2 by water splitting/generation of photogenerated free radicals (radical hydroxide/superoxide)[3-5]. The efficiency of photocatalyst depends on many factors like band gap, morphology (structure, surface area) etc. which inturn influences electronic, optical properties, thus affecting light harvesting nature of photocatalyst[6-11]. Semiconductor photocatalysts have proven wide applicability in above areas as they lead to the degradation of organic pollutants into CO_2, H_2O, and other moieties at room temperature conditions[12].

Among a class of these photocatalysts, Zn based semiconductor like zinc selenide (ZnSe), with wide direct band gap (2.67 eV) and large (21 meV) exciton binding energy[13-15] finds an important place as photocatalyst[16-20]. Similarly, the core-shell structures[21-27] on a nanometer scale can serve as efficient since the shell can affect charge, functionality, the reactivity of surface, which results in stability and dispersibility of core. Shell material can impart the core particles properties like optical, catalytic, bioconjugation and non-toxicity for use in optics, pharmaceuticals, catalysts, biology, and drug delivery[28-32]. SiO_2 is a favorable material for shell structure as its preparation, environmental stability and compatibility with other materials is high, so silica (non-toxic) was selected for shell structure around ZnSe, to study optical and photocatalytic activity on MB solution.

This work is an extended part of our previous work[33], now carried on ZnSe NPs, to provide comparative studies of optical properties and photodegradation of MB under room temperature conditions. The results will provide an insight in selection of more efficient photocatalytic system (silica coated, CdSe/ZnSe). Synthesis of SZNPs was performed through sol-gel technique, whereas template, i.e. ZnSe NPs were prepared by chemical co-precipitation. Different samples were synthesized by changing silica (TEOS) concentration by taking different mass to volume ratio of ZnSe:TEOS, i.e. mass to mass ratio of ZnSe:SiO_2 ranging from 0.0267 to 0.1071. Photodegradation experiments on MB by ZnSe and SZNPs (different mass ratio samples) were

*Corresponding author (E-mail: maheshverma08@gmail.com)

performed by comparision of absorption intensity with time for varried samples for optimal of silica coating determination. Mechanism and reaction kinetics of photodegradation of bare and SZNPs have been discussed, along with the recyclic experiments of SZNPs on MB. Degradation efficiency was calculated by performing series of successive photodegradation measurements, and its reuse at each cycle with MB solution (fresh) after its recovery from experiment.

2 Experimental

Chemicals required: zinc chloride ($ZnCl_2$), selenium powder (Se), sodium borohydride ($NaBH_4$), potassium hydroxide (KOH), thioglycolic acid (TGA), ethanol, NH_4OH, and MB were purchased from HPLC, Himedia Chemicals, Avantor Performance Materials India and Sigma Aldrich company.

SZNPs were prepared in two steps: first synthesis of core, i.e., ZnSe then involving coating of silica shell, i.e., SiO_2 around core part.

2.1 Synthesis of ZnSe NPs

Chemical co-precipitation method with some modifications[34] was adopted. Zinc chloride (3 g), was added to DI water under stirring until dissolved, 2 mL TGA (capping agent) was added to the solution under stirring. NaHSe solution (reaction of 0.4 g of Se with 0.72 g of $NaBH_4$ in DI water) was injected in the above solution, formation of yellow colour solution was noticed, this solution was refluxed for 3 h at temperature and pH values of 90 °C and 9 (using KOH). Precipitate was washed with DI water/ethanol and dried in vacuum at 65 °C for more than 48 h. The plausible reaction mechanism can be given by:

$$4NaBH_4 + 2Se + 7H_2O \rightarrow 2NaHSe + Na_2B_4O_7 + 14H_2\uparrow \quad \ldots (a)$$

$$NaHSe + ZnCl_2 \rightarrow ZnSe + NaCl + HCl \quad \ldots (b)$$

2.2 SiO_2 coating over ZnSe NPs

Silica coating on ZnSe NPs was performed by sol-gel method, typically 0.1 g of ZnSe NPs was suspended to 50 mL of ethanol under sonication, and then 0.06 g of cetyltrimethyl ammonium bromide (CTAB), was added to it. Afterwards, 10 mL of NH_4OH and different volumes of tetraethyl orthosilicate (TEOS) varying from 1 to 4 mL were added to solution (under sonication for 4 h) for obtaining different samples of mass: volume ratio of ZnSe:TEOS, i.e., ZnSe:SiO_2 mass ratio (0.0267 to 0.1071). The precipitate was washed with ethanol and DI water, and vacuum dried at 60 °C for 4 h for carrying out various characterizations.

2.3 Material characterization

Determination of crystal structure and phase of the as-prepared sample was carried out by using Panalytical Xpert Pro X-ray Diffractometer (λ = Cu-K_α i.e.1.5418 Å). SEM (Carl Zeiss EVO 18) and TEM (Tecnai 20 G^2 S-Twin) were used to study the surface morphology and particle size of samples. FTIR (IR Affinity, Shimadzu) and UV-Vis spectrophotometer (Agilent Cary 5000 series) were used to identify chemical groups, absorption spectra of sample. PL and Raman measurements were conducted on LS 55-Perkin-Elmer and micro-Raman STR 300 (Airix Corporation/ TechnoS Instruments) having Ar^+ ion laser as a source at 532 nm wavelength (2.2 eV).

2.4 Photocatalytic measurements

MB as supplied was used for photocatalytic degradation experiments, under irradiation source of 500 W high-pressure mercury lamp conducted at room temperature. A constant distance of 15 cm was adjusted between lamp and reactor vessel, fitted with water circulation arrangement for maintaining temperature of vessel. 50 mL of 10 mg/L concentration of MB solution was taken and 50 mg as synthesized ZnSe/SiO_2, i.e., photocatalyst and was added to it under constant stirring with pH adjusted to 7. This reaction solution was stirred for 35 min for adsorption-desorption equilibrium process taking place between dye and photocatalyst. The remaining MB concentration after adsorption-desorption equilibrium (C_o) and during photodegradation (C) was evaluated from change in intensity of UV-Vis absorption peak of the solution observed at 664 nm. Definite quantity solution was taken out at regular time intervals of 10 min, containing photocatalyst (exposed to light) for monitoring the intensity of UV absorption peak. Degradation efficiency was calculated using the following equation[35]:

$$\text{Degradation (\%)} = ((C_o - C)/C_o) \times 100 = ((A_o - A)/A_o) \times 100 \quad \ldots (1)$$

Where C_o, C, A_o and A being the initial concentration, changed concentration, initial absorbance, and changed absorbance of MB solution at characteristic absorption wavelength of 664 nm.

3 Results and Discussion

3.1 Phase, morphology and micro-structural (XRD, FTIR, SEM and TEM)

XRD patterns of ZnSe NPs and SZNPs are shown in Figure 1a. Diffraction peaks corresponding to 2θ values of 23.29°, 24.95°, 27.41°, 35.13° and 41.19° correspond to various planes (100), (002), (101),

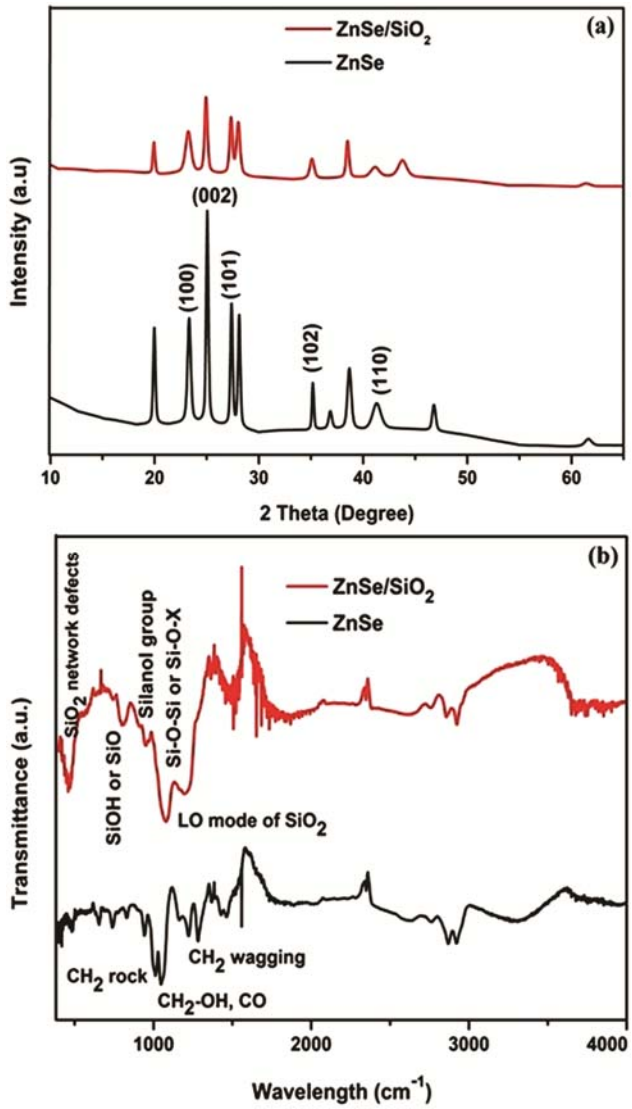

Fig. 1 — (a) XRD pattern of ZnSe and SZNPs and (b) FTIR spectra of ZnSe and SZNPs showing chemically bonded groups.

(102) and (110) of ZnSe, having hexagonal crystal system with lattice parameters, a = 4.32 (Å), b = 4.34 (Å) and c = 7.0 (Å). The size of the crystallite calculated by Debye Scherrer relation was found to be 10 nm:

$$D = \frac{0.9\lambda}{\beta cos\theta} \qquad \ldots (2)$$

In the above relation D is the crystallite size, λ wavelength of Cu-Kα, β full width at half maximum and θ is the angle corresponding to diffraction peaks. XRD diffraction peaks of SZNPs are found similar to ZnSe XRD pattern, except variation in intensity and disappearance of some peaks. Figure 1 (a) which refers to the formation of silica coating on ZnSe NPs. The crystallite size of SZNPs calculated using above relation was found to be 14 nm.

FTIR spectra of ZnSe NPs and SZNPs is shown in Fig.1 (b), which shows the presence of CH_2-OH, CO, CH_2, and CH_2 groups at 1055 cm^{-1}, 999 cm^{-1} and at 1290 cm^{-1}, respectively. The presence of silica attached to SZNPs can also be found in Fig. 1 (b), like stretching of SiO_2 network[33] at 470 cm^{-1}, silanol groups at 944 cm^{-1}, stretching vibrations of Si-O-Si/ Si-O-X [36, 37], (X=ethoxy group) at 1068 cm^{-1} and TO or LO mode of high frequency vibration corresponding to SiO_2[37] at 1182 cm^{-1}. Band at 820 cm^{-1} has been assigned to stretching vibration of Si-OH/Si-O groups. All these results confirm the silica coating on ZnSe NPs probably forming shell type structure.

TEM micrographs of ZnSe and SZNPs are shown in Fig. 2 (a, b) depicting varying size of SZNPs, having an average size between 8-10 nm, which being in good agreement with XRD results. SAED pattern in Fig. 2 (b) shows amorphous nature of SZNPs due to silica coating on ZnSe NPs. EDAX fitted with TEM was used for elemental mapping of SZNPs, it shows the presence of elements like Si, O, Zn and Se which confirms silica coating on ZnSe NPs, (Fig. 2 (c)). The peaks at around 2 and 8 keV in the EDAX spectrum are K_α values of carbon and copper which (0.277 and 8.04 keV) which is as a result of sample deposited on carbon-coated copper grids. SEM micrograph of SZNPs shows the unsymmetrical geometry of particles which can be related to agglomeration of core (ZnSe) during silica coating process in Fig. 2 (d).

3.2 Optical properties (UV, PL and Raman studies)

Figure 3 (a) shows the UV-Vis absorption spectra of ZnSe NPs and SZNPs, with absorption peaks located at 303, 321 nm, and 304, 324 nm. Shift in absorption edge of SZNPs towards the higher wavelength side along with decrease in intensity compared to ZnSe NPs can be noted as result of silica coating. Band gap was calculated using Tauc relation[38]:

$$\alpha h\nu = A(h\nu - E_g)^n \qquad \ldots (3)$$

where ν, α, h and E_g are frequency, absorption coefficient, Planck's constant and band gap. The value of exponent term n= ½ has been used for direct band gap ZnSe NPs. Band gap calculated by extrapolation of linear part of graph $(\alpha h\nu)^2$ versus hν gives a value of 3.1 and 3.7 eV for ZnSe and SZNPs (Fig. 3 (b)). This shows that the silica coating process has increased the band gap energy of ZnSe NPs.

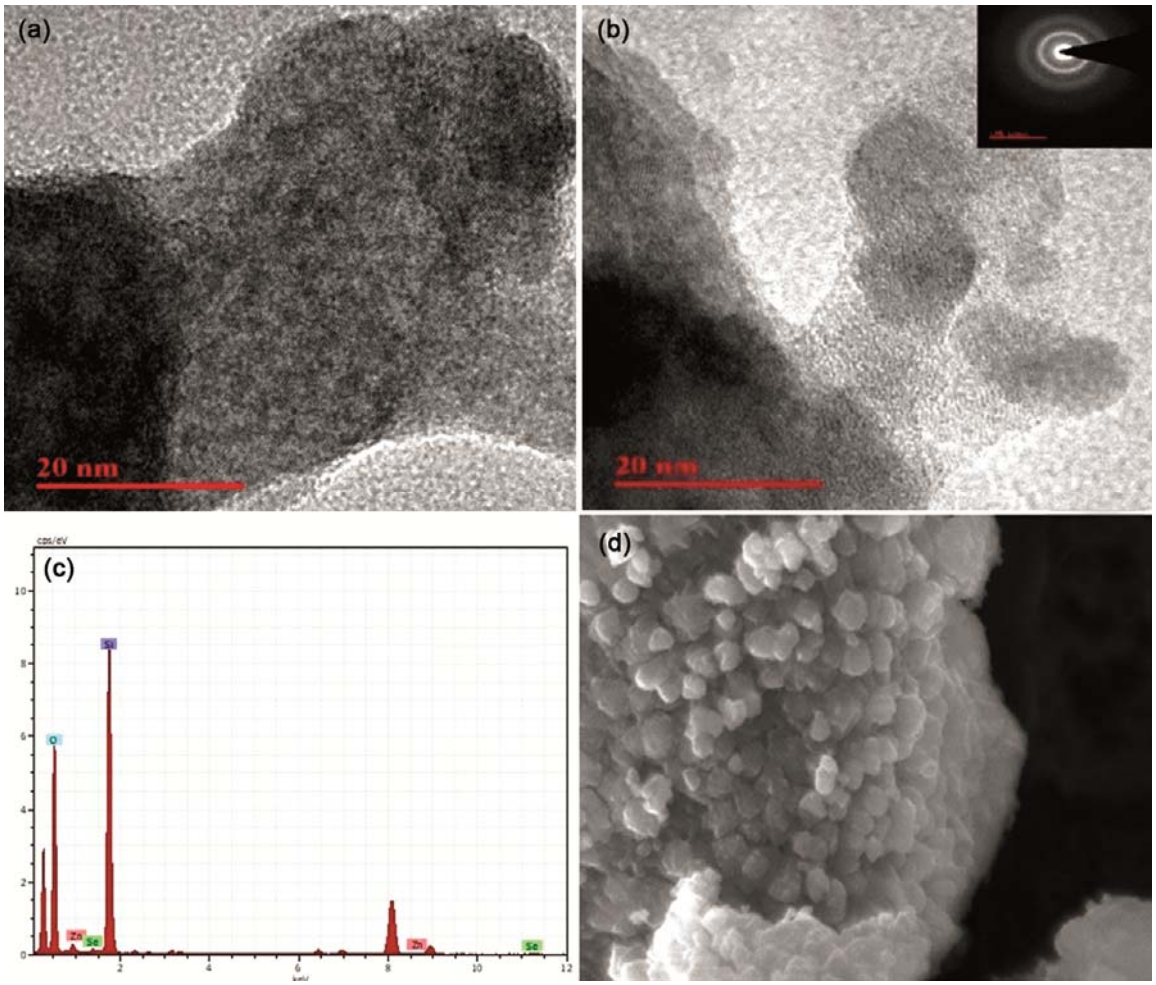

Fig. 2 — (a) TEM micrographs of ZnSe, (b) of SZNPs along with and SAED pattern (inset), (c) EDAX of SZNPs and (d) SEM micrograph of SZNPs.

Silica being a non-luminescent material, photoluminescence behavior of mesoporous silica/ silica NPs are explained by siloxane groups, defects, surface states, or non-connecting oxygen groups (red bands)[39, 40]. PL spectra of ZnSe and SZNPs nanoparticles were taken at room temperature (Fig. 3 (c)), to study the separation of photogenerated charge carriers which shows narrow emission at 420 nm for ZnSe NPs and a red shift of 8 nm, i.e., 428 nm for SZNPs. Increase in FWHM of PL peak can be related to different surface states of ZnSe NPs and SZNPs. Intensity variation and red shift are attributed to silica coating, generation of trap states/recombination centers, and due to less direct recombination of charge carriers from the valence band to conduction band as result of silica coating. These factors directly influence the electronic properties of ZnSe core, i.e., re-absorption by larger nanoparticles in the cluster, as the PL arising from the smaller cluster is followed by larger clusters. This is due to aggregation of core (ZnSe) inside the silica spheres during surface modification (silica coating) process[41, 42]. Also change in refractive index of the material, broadening of electronic transitions due to silica coating and chemical reaction during silanization process[43] may be a probable reason.

Raman spectroscopy gives direct information about molecular/phonon vibration, excitation and chemical bonding of any material. Raman spectrum of SZNPs is shown in Fig. 3 (d), the peak at 197 cm^{-1} represents TO mode of ZnSe[44]. Raman bands at 742 and 452 cm^{-1}, represents the Si-O-Si symmetrical stretching and network bending modes[45-47] whereas bands present at 947 and 655 cm^{-1} correspond to surface stretching mode and D2 defect mode of Si-OH[45-48]. Peaks located at 1021 and 1142 cm^{-1} represent transverse-optical (TO) and longitudinal-optical (LO) modes[45] of silica groups. Thus the above results confirm the silica coating on ZnSe NPs.

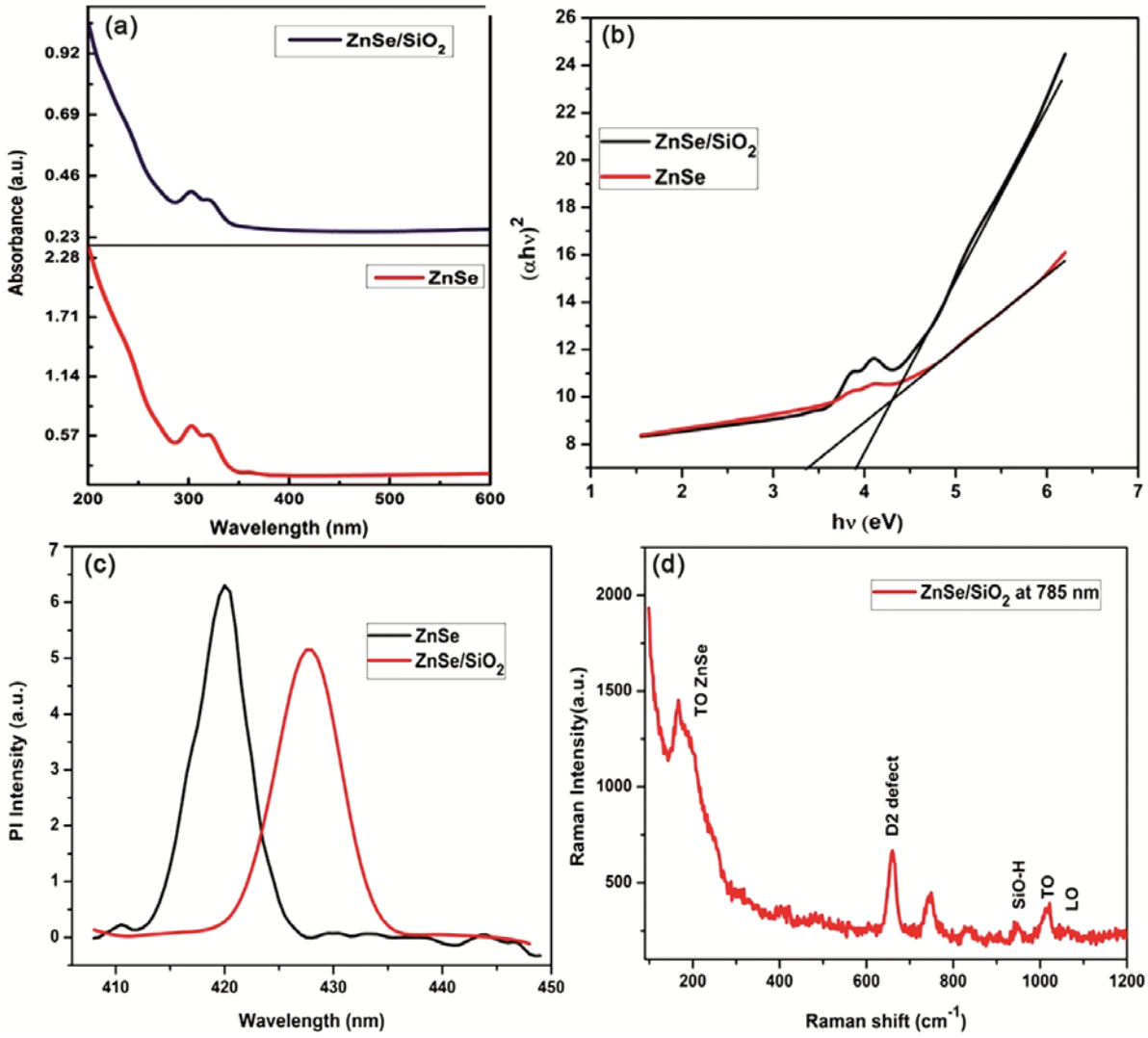

Fig. 3 — (a) UV-Vis absorption spectra of ZnSe and SZNPs, (b) Tauc relation plot for band gap determination of ZnSe and SZNPs, (c) PL spectra of ZnSe and SZNPs and (d) Raman spectrum of SZNPs showing presence of silica coating on ZnSe NPs.

3.3 Photodegradation of MB solution and kinetics of mechanism

Photocatalysis being a surface phenomenon, hence the surface of photocatalyst[49] plays an important role in influencing the photodegradation process. Therefore, adsorption of MB from solution onto the surface of ZnSe and SZNPs is of great interest. In order to study this behavior, adsorption equilibrium of MB was first achieved in dark conditions with catalyst, and C_o was measured, which is the actual dye concentration as compared to feed dye solution, before the beginning of irradiation process. Photodegradation of dye molecule takes place through photo-absorption of light by the photocatalyst, which gives rise to electrons and holes required for the transfer of charge; finally, these charge carriers are used by the reactants leading to degradation. The factors affecting the photocatalysis of dye in the presence of semiconductors involves: firstly, the formation electrons and holes in the conduction and valence band due to light-irradiation, secondly due to electron-hole pair recombination. Charge separation and recombination process determine the photocatalysis efficiency of a photocatalyst in bulk and on the surface areas. PL spectra can be used to determine charge recombination rate[50] between two different energy states, so higher the PL intensity, more is recombination rate of photogenerated electrons and holes leading to lower photocatalytic process. Surface area of photocatalyst also plays an important role in shaping photoactivity[51] because more species get absorbed to active sites. Thereby

leading to degradation of more dye species, which forms a probable explanation in our study as silica coating onto ZnSe increases its surface area and active sites.

The UV-Vis absorption band for degradation of MB by ZnSe and SZNPs (mass ratio of ZnSe:SiO_2, i.e. 0.0535), is shown in Fig. 4 (a, b). Gradual decrease of absorbance at 664 nm for MB with irradiation time can be noted. The absence of hypochromic shift in Fig. 4 (a, b) indicates absence of the degradation intermediate. Photodegradation efficiency of samples, with different silica coating

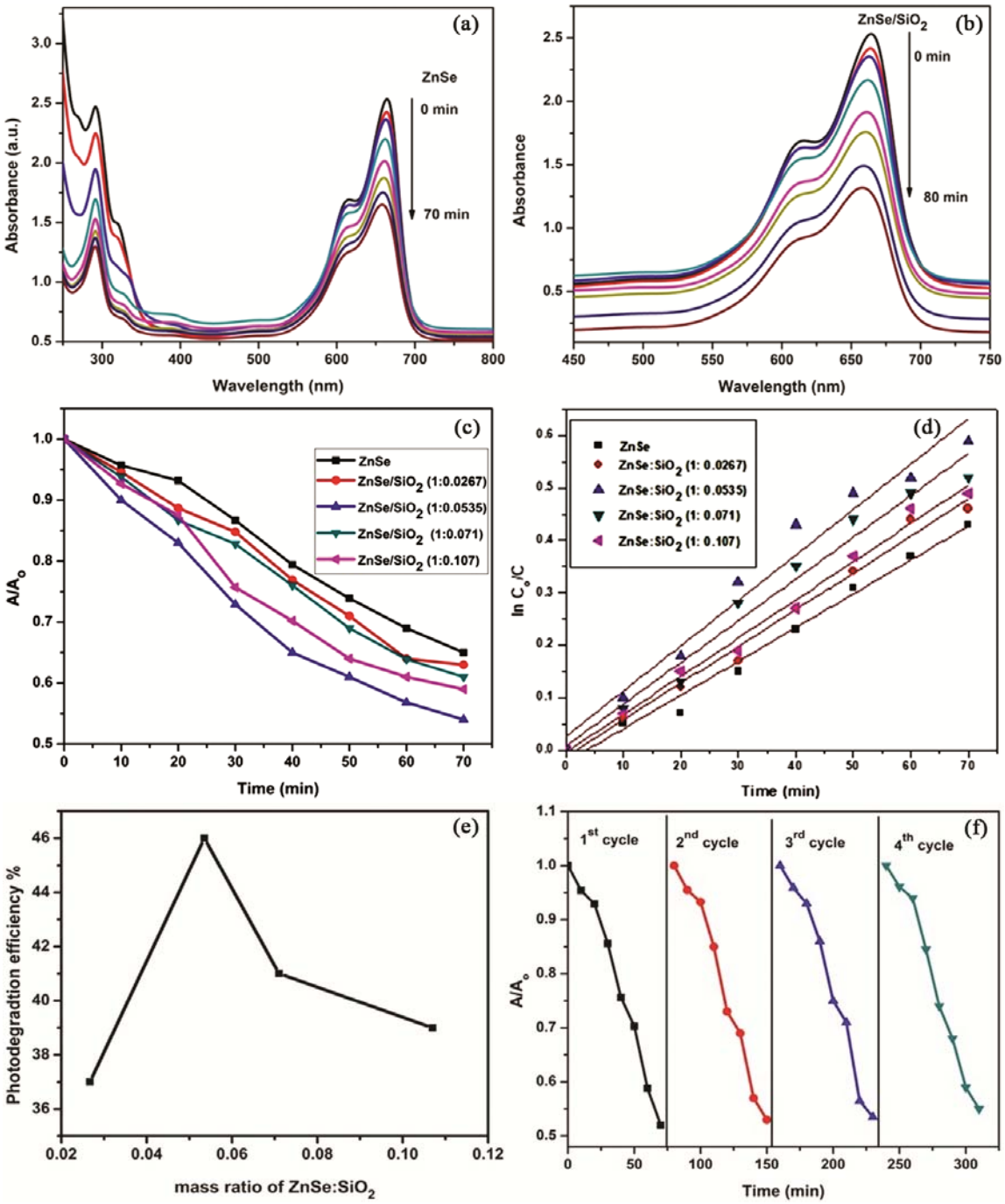

Fig. 4 — (a, b) Plot of photodegradation of MB by ZnSe and SZNPs, (c) degradation of absorption peak (A_o/A) of MB by ZnSe and SZNPs as a function of irradiation time, (d) plot of ln (C_o/C) with time t (min) of ZnSe and SZNPs, for determining the rate of reaction, (e) plot of photodegradation efficiency vs. mass ratio of ZnSe:SiO_2, and (f) Recyclic use of SZNPs (mass ratio 0.0535) after every recovery.

(varying TEOS volume) has been plotted in Fig. 4 (c), i.e., A/A_o versus time. Here, A is the absorbance value of MB at each irradiation time at 664 nm and A_o is the absorbance value before irradiation, i.e. at t = 0, when adsorption and desorption equilibrium was established. It shows that on increasing amount of SiO_2 coating (mass ratio) on ZnSe from 0.0267 to 0.0535 leads to an increase in photodegradation efficiency. On further increasing the silica content in coating process (0.071 to 0.107), photodegradation of MB decreases, which reflects that photodegradation is caused by ZnSe, not by SiO_2[52].

Reaction kinetics and reaction rates for the dyes degradation at low concentration solutions are explained by Langmuir-Hinshelwood (L-H) equations[53-56]. Reaction rate constants (K) were obtained for ZnSe and SZNPs samples by plotting ln (C_o/C) as a function of the irradiation time (t) for degradation of MB by ZnSe and SZNPs NPs as shown in Fig. 4 (d). C_o and C are initial concentration (t=0) and at time 't'. Pseudo-first order reaction behavior is found from the semi-logarithmic plot (linear line) passing through the origin[57].

$$\ln C_o/C = K\,t \quad \ldots (4)$$

Where factor K represents rate constant of reaction obtained from the slope of above Eq.(4), its value for different samples are listed in Table 1. Figure 4 (e) shows the degradation efficiency of MB by ZnSe and SZNPs samples of different mass ratio of $ZnSe:SiO_2$ (0.1071 to 0.0535) with degradation efficiency % plotted on Y axis versus concentration (mass ratio of $ZnSe:SiO_2$) on X-axis, Highest photodegradation of MB was found to be 46 % with sample having mass ratio $ZnSe:SiO_2$, i.e., 0.0535.

From the results of kinetic study of MB degradation by ZnSe and different SZNPs samples different mass ratio of $ZnSe:SiO_2$, i.e., 0.1071 to 0.0535 are shown in Table 1. It can be noted that as the concentration of SiO_2 increases in coating process, photodegradation efficiency increases, leading to an increase in the rate constant, highest being observed for the mass ratio of $ZnSe:SiO_2$ equal to 0.0535 sample, reaction mechanism can be represented as under:

$$h\nu + ZnSe \rightarrow ZnSe\,(e^-_{CB} + h^+_{VB}) \quad \ldots (5)$$

$$h^+_{VB} + MB \rightarrow \text{oxidation of MB} \quad \ldots (6)$$

$$h^+_{VB} + H_2O \rightarrow H^+ + *OH \quad \ldots (7)$$

$$h^+_{VB} + OH^- \rightarrow *OH \quad \ldots (8)$$

Electron-hole pairs are generated on the surface of photocatalyst, i.e., ZnSe, giving rise to reactive intermediate by oxidation of MB. Reaction of a hole (h^+_{VB},) with OH^- or decomposition of water leads to generation of hydroxyls though degradation of dye. Reduction of O_2 by the electrons in the conduction band (e^-_{CB}) gives rise to superoxide anion, forming organic peroxides.

$$e^-_{CB} + O_2 \rightarrow *O_2^- \quad \ldots (9)$$

$$*O_2^- + MB \rightarrow MB(*OO) \quad \ldots (10)$$

$$*O_2^- + H^+ \rightarrow HO_2^* \quad \ldots (11)$$

$$*O_2^- + HO_2* + H^+ \rightarrow H_2O_2 + O_2 \quad \ldots (12)$$

$$H_2O_2 \rightarrow 2*OH \quad \ldots (13)$$

$$MB + *OH \rightarrow \text{degradation products} \quad \ldots (14)$$

The electrons in conduction band produces hydroxyl radicals, which is the main cause of the degradation of the organic material, dye (Eq. 14).

The recyclic photocatalytic behavior of SZNPs ($ZnSe:SiO_2$, i.e. 0.0535) is shown in Fig. 4 (f), for successive reuse the sample was treated with distilled water after every cycle of use, followed by drying at 120 °C in vacuum oven for its use with fresh MB solution in each cycle. After the 4th cycle of successive use a decrease of only 7% was noted, this reflects efficacy of SZNPs in the degradation of MB. A schematic representation for the degradation MB solution by ZnSe NPs is shown in Fig. 5. Thus it can

Table 1 — Showing variation of photodegradation efficiency and reaction kinetics with varied mass ratio of silica coating on ZnSe NPs.

Sample	Mass ratio of $ZnSe:SiO_2$	Photodegradation Efficiency (%)	Value of rate constant (K) min^{-1}
(a) ZnSe	1.0000:0.0000	35	6.4×10^{-3}
(b) SZNPs	1.0000:0.0267	37	7×10^{-3}
(c) SZNPs	1.0000:0.0535	46	8.6×10^{-3}
(d) SZNPs	1.0000:0.0710	41	7.9×10^{-3}
(e) SZNPs	1.0000:0.1071	36	7.2×10^{-3}

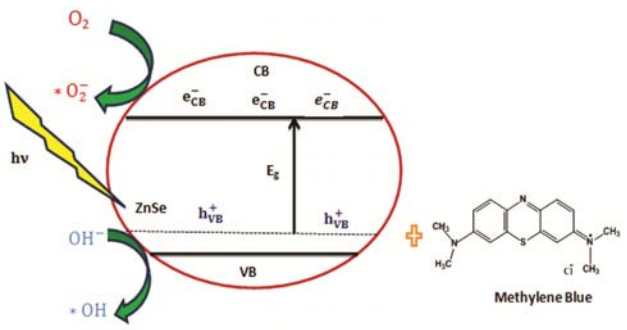

Fig. 5 — Mechanism for degradation of MB solution by ZnSe nanoparticles.

be said that optimal silica coating is necessary for achieving high degree of photodegradation of MB solution by SZNPs. Also as silica being a good binder, easy recovery of catalyst is possible after every use by washing followed by heating without much loss in optical properties of ZnSe. Thus this work emphasis the role of optimal silica coating on ZnSe NPs (photocatalyst), which can be further extended to other optical materials.

4 Conclusions

Photodegradation studies of MB by ZnSe and SZNPs (varying mass ratios of $ZnSe:SiO_2$) were conducted. Photodegradation mechanism of MB by SZNPs follows a pseudo-first order reaction kinetics, due to linear behavior of plot of $\ln(C_o/C)$ versus irradiation time. Result showed that an optimal silica coating (mass ratio of $ZnSe:SiO_2$ equal to 0.0535) is necessary for achieving high degree of photocatalytic efficiency and rate constant i.e. 8.6×10^{-3} min^{-1} for $ZnSe:SiO_2$ (1.0000:0.0535) sample. Recyclic efficiency of this sample after 4^{th} cycle of reuse was almost constant thereby showing the efficacy of SZNPs in the photodegradation of MB solution.

Acknowledgement

Authors gratefully acknowledge the financial grant received from UGC, New Delhi (India) in the from of Emeritus Fellow to Prof N S Saxena They also extend their thanks to Mr Gagan Choudhary, Dy Director, GTL, Jaipur for Raman measurements.

References

1 Pettyjohn W A & Hounslow A W, *Groundwater Monit Remediat*, 3 (1983) 41.
2 Gokul P, Vinoth R, Neppolian B & Anandhakumar S, *Appl Surf Sci*, 418 (2017) 119.
3 Harish S, Archana J, Navaneethan M, Silambarasan A, Nisha K D, Ponnusamy S, Muthamizhchelvan C, Ikeda H, Aswal D K & Hayakawa Y, *RSC Adv*, 6 (2016) 89721.
4 Zhang Z, Long J, Yang L, Chen W, Dai W, Fu W & Wang X, *Chem Sci*, 2 (2011) 1826.
5 Ding Y & Nagpal P, *Phys Chem Phys*, 19 (2017) 10042.
6 Guo X, Qin X, Xue Z, Zhang C, Sun X, Hou J & Wang T, *RSC Adv*, 6 (2016) 48537.
7 Ayodhya D & Veerabhadram G, *Mater Today Energy*, 9 (2018) 83.
8 Moshfegh A Z, *J Phys D: Appl Phys*, 42 (2009) 233001.
9 Liu R, Sun Z, Song X, Zhang Y, Xu L & Xi L, *Appl Catal A: Gen*, 544 (2017) 137.
10 Huang Q, Zhang Q, Yuan S, Zhang Y & Zhang M, *Appl Surf Sci*, 353 (2015) 949.
11 Huang Y, Xu Y, Zhang J, Yin X, Guo Y & Zhang B, *J Mater Chem A*, 3 (2015) 19507.
12 Romao J & Mul G, *ACS Catal*, 6 (2016) 1254.
13 Goswami B, Pal S, Ghosh C & Sarkar P, *J Phys Chem C*, 113 (2009) 6439.
14 Philipose U, Ruda H E, Shik A, Souza C F D & Sun P, *J Appl Phys*, 99 (2006) 066106.
15 Anpo M, Dohshi S & Kitano M, *Ann Rev Mater Res*, 35 (2005) 1.
16 Verma M, Gupta D K, Patidar D, Sharma K B & Saxena N S, *Adv Sci Lett*, 21 (2015) 2657.
17 Verma M, Kaswan A, Patidar D, Sharma K B & Saxena N S, *J Mater Sci: Mater Electron*, 27 (2016) 8871.
18 Bharati B, Sonkar A K, Singh N, Dash D & Rath C, *Mater Res Express*, 4 (2017) 085503.
19 Li S, Lin Q, Liu X, Yang L, Ding J, Dong F, Li Y, Irfana M & Zhang P, *RSC Adv*, 8 (2018) 20277.
20 Azeez F, Hetlani E A, Arafa M, Abdelmonem Y, Nazeer A A, Amin M O & Madkour M, *Sci Reports*, 8 (2018) 7104.
21 Cao H, Xiao Y & Zhang S, *Nanotechnology*, 22 (2011) 015604.
22 Zhang L, Yang H, Xie X, Zhang F & Li L, *J Alloy Compd*, 473 (2009) 65.
23 Chan W C & Nie S, *Science*, 281 (1998) 2016.
24 Schneider J J, *Adv Mater*, 13 (2001) 529.
25 Lee H B, Yoo Y M & Han Y H, *Scripta Mater*, 55 (2006) 1127.
26 Zhang L, Acunzi M D & Kappl M, *Langmuir*, 25 (2009) 2711.
27 Wang S, Cao H, Gu F, Li C & Huang G, *J Alloys Compd*, 457 (2008) 560.
28 Gupta D K, Verma M, Gopal R, Sharma K B & Saxena N S, *Indian J Pure Appl Phys*, 56 (2018) 970.
29 Verma M, Gupta D K, Patidar D, Sharma K B & Saxena N S, *Adv Sci Lett*, 22 (2016) 3790.
30 Li J, Cao C & Zhu H, *Diam Relat Mater*, 16 (2007) 359.
31 Le Y, Pu M & Chen J, *J Non-Cryst Solids*, 353 (2007) 164.
32 Gharibe S, Afshar S & Vafayi L, *Afr J Pharm Pharmaco*, 5 (2011) 2265.
33 Verma M, Sharma K B & Saxena N S, *J Mater Sci Mater Electron*, 27 (2016) 11248.
34 Verma M, Patidar D, Sharma K B & Saxena N S, *J Inorg Organomet Polym*, 26 (2016) 75.
35 Xu J, Chang Y, Zhang Y, Ma S, Qu Y & Xu C, *Appl Surf Sci*, 255 (2008) 1996.
36 Brinker C L & Scherer G W, *Sol-gel Science*: *The Physics and Chemistry of Sol-gel Processing*, (Academic Press New York) 581 (1990).
37 Que W, Zhou Y, Lam Y L, Chan Y C & Kam C H, *Thin Solid Films*, 358 (2000) 16.
38 Seoudi R, Shabaka A, Eisa W H, Anies B & Faraje N M, *Physica B*, 405 (2010) 919.
39 Glinka Y D, Lin S H, Hwang L P & Chen Y T, *Appl Phys Lett*, 77 (2000) 3968.
40 Glinka Y D, Zyubin A S, Mebel A M, Lin S H, Hwang L P & Chen Y T, *Eur Phys J D*, 16 (2001) 279.
41 Jin L, Yu D D, Liu Y, Zhao X L & Zhou J G, *Talanta*, 76 (2008) 1053.
42 Yang Y H & Gao M Y, *Adv Mater*, 17 (2005) 2354.
43 Rogach A L, Nagesha D, Ostrander J W, Gierig M, Kotov N A, Bun R, *Chem Mater*, 12 (2000) 2676.
44 Verma M, Patidar D, Sharma K B & Saxena N S, *J Nanoelectron Optoelectron*, 10 (2015) 320.
45 Galeener F L & Mikkelsen J C, *Phys Rev B*, 23 (1981) 5527.

46 Brinker C J, Kirkpatrick R J, Tallant D R, Bunker B C & Montez B, *J Non-Cryst Solids*, 99 (1988) 418.
47 McMillan P, *American Mineral*, 69 (1984) 622.
48 Galeener F L & Geissberger A E, *Phys Rev B*, 27 (1983) 6199.
49 Jang Y J, Simer C & Ohm T, *Mater Res Bull*, 41(2006) 67.
50 Chen L, Zhang W, Feng C, Yang Z & Yang Y, *Ind Eng Chem Res*, 51 (2012) 4208.
51 Reddy B M, Sreekanth P M, Yamada Y & Kobayashi T, *J Mol Catal A Chem*, 227 (2005) 81.
52 Ismail A, Ibrahim I & Mohamed R, *Appl Catal B*, 45 (2003) 161.
53 Segota S, Curkovic L & Ljubas D, *Ceram Int*, 37 (2011) 1153.
54 Daneshvar N, Rabbani M, Modirshahla N, *J Photochem Photobiol A*, 168 (2004) 39.
55 Chong M N, Jin B & Chow C W K, *Water Res*, 44 (2010) 2997.
56 Bizarro M, Rodriguez M A T, Ojeda M L, *Appl Surf Sci*, 255 (2009) 6274.
57 Chen R G, Bi J H, Wu L, Li Z H & Fu X Z, *Cryst Growth Des*, 9 (2009) 1775.